

Identifying Global Anatomical Differences: Deformation-Based Morphometry

John Ashburner,* Chloe Hutton, Richard Frackowiak, Ingrid Johnsrude,
Cathy Price, and Karl Friston

Functional Imaging Laboratory, Wellcome Department of Cognitive Neurology,
Institute of Neurology, London, UK



Abstract: The aim of this paper is to illustrate a method for identifying macroscopic anatomical differences among the brains of different populations of subjects. The method involves spatially normalizing the structural MR images of a number of subjects so that they all conform to the same stereotactic space. Multivariate statistics are then applied to the parameters describing the estimated nonlinear deformations that ensue. To illustrate the method, we compared the gross morphometry of male and female subjects. We also assessed brain asymmetry, the effect of handedness, and interactions among these effects. *Hum. Brain Mapping* 6:348–357, 1998. © 1998 Wiley-Liss, Inc.

Key words: morphometrics; anatomy; spatial normalization; multivariate analysis



INTRODUCTION

In this paper we introduce a new technique to characterize differences among structural or anatomical brain images. The anatomical differences between any two brains can be expressed at a microscopic scale (e.g., differences in cytoarchitectonics or myeloarchitectonics), at a mesoscopic scale (e.g., cortical dysplasia), or at a macroscopic level (e.g., ventricular enlargement or abnormal temporal lobe asymmetry). From the perspective of neuroimaging, differences at a mesoscopic and macroscopic level are amenable to measurement. We recently developed a technique that looks for differences at a mesoscopic scale (i.e., several millimeters), called *voxel-based morphometry*, and we demonstrated it in relation to regionally specific abnormali-

ties in grey matter in schizophrenia [Wright et al., 1995]. This approach uses spatially normalized, segmented images in conjunction with statistical parametric mapping to provide inferences about differences in the local density of various tissue compartments (e.g., grey matter or white matter). Voxel-based morphometry throws away macroscopic or global differences in anatomy at the spatial normalization step. Here we describe a technique that characterizes these global differences in macroscopic anatomy that complements voxel-based morphometry, allowing one to examine differences at both mesoscopic and macroscopic scales.

By analogy with voxel-based morphometry, we called this new approach *deformation-based morphometry*. Both can be seen as developments in the growing field of computational neuroanatomy. Deformation-based morphometry is a characterization of the differences in the vector fields that describe global or gross differences in brain shape. These vector fields are the deformation fields used to effect nonlinear variants of spatial normalization, when one of the images is a template that conforms to some standard anatomical space. In

Contract grant sponsor: Wellcome Trust.

*Correspondence to: John Ashburner, Functional Imaging Laboratory, Wellcome Department of Cognitive Neurology, 12 Queen Square, London WC1N 3BG, UK. E-mail: j.ashburner@fil.ion.ucl.ac.uk

Received for publication 11 February 1998; accepted 5 June 1998

what follows we take the deformation fields that map a series of images onto the same template, and then compare them to see if there are any systematic differences. Because the deformation fields are multivariate, we employ standard multivariate statistical techniques to estimate the nature of the differences and to make inferences about them. The endpoint of deformation-based morphometry is a *P* value pertaining to the significance of the effect and one or more canonical vectors, or deformations, that characterize their nature. These results are obtained using multivariate analysis of covariance (ManCova) and canonical variates analysis (CVA), respectively.

The importance of this technique is that it is completely automated and therefore completely reproducible. Its validity is established in terms of the estimation of the deformation fields and the templates used in the analysis. Also, there is no implicit bias in terms of which anatomical differences might be identified.

Studies of brain morphometry have been carried out by many researchers on a number of different populations, including patients with schizophrenia, autism, dyslexia, and Turner's syndrome. In relation to schizophrenia, much of the work has focused on the dimensions of the temporal lobes [Crow, 1990; Bartzokis et al., 1996; Jacobsen et al., 1996], hippocampal volumes [Suddath et al., 1990; Altshuler et al., 1990], ventricle volumes [Suddath et al., 1990; Blackwood et al., 1991; Lieberman et al., 1992], anterior cingulate and frontal lobes [Noga et al., 1995; Nopoulos et al., 1995], basal ganglia [Frazier et al., 1996], and whole brain volumes. Other areas of research include sexual dimorphism of schizophrenic brains [Nasrallah et al., 1990] and the degree of asymmetry [Crow, 1990]. Abnormal cerebellar morphology has been found in autism [Ciesielski and Knight, 1994], along with differences in the morphology of the forebrain, especially the anterior ventricular horns, lateral ventricles, and right ventricular nucleus [Gaffney et al., 1989]. Autistic brains have also been found to be more symmetric than control brains [Tsai et al., 1983]. Differences found in Turner's syndrome include smaller volumes of a number of brain structures [Murphy et al., 1993], and different regional distributions of grey and white matter in both right and left parietal regions [Reiss et al., 1995].

Often, the morphometric measurements used in these studies have been obtained from brain regions that can be clearly defined, resulting in a wealth of findings pertaining to these particular measurements. These measures are typically volumes of unambiguous structures such as the hippocampi or ventricles. However, there are a number of morphometric features that may be rather more difficult to quantify by inspection,

meaning that many structural differences may be overlooked. In summary, the study of macroscopic anatomical dimorphism is an important field that has provided a number of intriguing insights into the pathogenesis or neuro-developmental aspects of several neuropsychiatric disorders. However, it is the case that most studies to date have focused on anatomical "metrics" that are easy to measure. These may, or may not, be germane to the pathophysiology under investigation. The importance of the approach described here is that it is not biased in any way to one particular structure or tissue, and gives an evenhanded and comprehensive assessment of anatomical differences throughout the brain.

Friston et al. [1995b] observed that, "The topography of an image can be characterized in terms of the coefficients corresponding to the spatial basis functions. This simple list of coefficients, taken in conjunction with the reference image, is a complete specification of the original image (down to the resolution imposed by the basis functions). The importance of this observation is that anatomical topography can be characterized by a multivariate measure (the coefficients) and subject to conventional multivariate statistics." What follows is an implementation of that basic idea.

In order to demonstrate the technique, we chose to study dimorphism in relation to handedness and sex. This should be seen as a vehicle to explain and illustrate how to do these analyses. The details of the statistical analysis are presented in Appendix A for the interested reader, and represent standard methods that have already been applied to functional imaging data [Friston et al., 1995a].

METHODS

High-resolution structural T1 MR images were acquired from 61 normal, healthy volunteers. These were all acquired on the same 2 Tesla Siemens Magnetom Vision scanner, using an MPRAGE sequence. The resolution of the images was $1 \times 1 \times 1.5$ mm. The data consisted of 15 female right-handed subjects, 5 female left-handed subjects, 30 male right-handed subjects, and 11 male left-handed subjects, all between ages 20–37. The scans were all acquired as part of ongoing functional imaging projects within the department, and all subjects had no neurological or psychiatric history.

The images were spatially normalized by a least-squares match to a template image. This template consisted of an average of 12 12-parameter affine-registered T1 MR images of the head, and was rendered symmetric (so that it could be used to examine

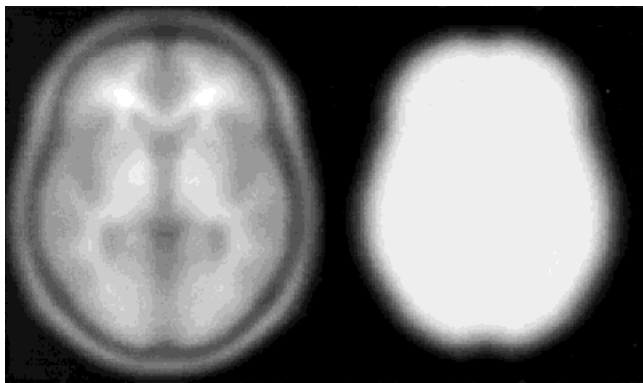


Figure 1.

The template (left) and weighting image (right) used by the registration. Note that the images have been smoothed using an 8-mm full-width at half-maximum isotropic Gaussian kernel in order to facilitate the registration.

brain asymmetry) by averaging with itself reflected across the sagittal midplane. The MRI sequence used to generate the images, constituting the template, was identical to that used for all the other images, thus ensuring that more accurate registrations could be achieved.

The first step of the normalization was to determine the optimum 12-parameter affine transformation [Ashburner et al., 1997]. Initially, the registration was performed by matching the whole of the head (including the scalp) to the template. Following this, the registration proceeded by only matching the brains together, by appropriate weighting of the template voxels (Fig. 1). This is a completely automated procedure (that does not require “scalp editing”) that discounts the confounding effects of skull and scalp differences.

The affine registration was followed by estimating nonlinear deformations, whereby the deformations were defined by a linear combination of three-dimensional discrete cosine transform (DCT) basis functions [Ashburner and Friston, 1998; Friston et al., 1995b]. Each of the deformation fields was described by 1,176 parameters, which represented the coefficients of the deformations in three orthogonal directions. The matching involved simultaneously minimizing the membrane energies of the deformation fields and the residual squared difference between the images and template, as described previously. The mean of the spatially normalized images is shown for each group in Figure 2. It can be seen that in terms of gross anatomy, following normalization, they are virtually indistinguishable.

Each set of spatial normalization parameters (affine and nonlinear) encodes a deformation field relating to the position, size, and shape of the brain. For the analysis presented here, we used only the information

relating to the shapes of the brains, by removing the effects of size and position (see Appendix B).

Following this, a matrix A_0 was generated, where each row contained the coefficients of the nonlinear basis functions, describing the difference in shape between the template and each image. For the multivariate analysis that followed, it was necessary to reduce the number of these coefficients relative to the number of images. Principal component analysis was used to compact this information, such that about 96% of the variance of the nonlinear deformations was represented by 20 parameters for each image. This dimension reduction used singular value decomposition to decompose matrix A_0 into unitary matrixes U_0 and V_0 , and diagonal matrix S_0 , such that $A_0 = U_0 S_0 V_0^T$. Matrix S_0 was reduced to a smaller diagonal matrix S , by eliminating the rows and columns containing the least important components. The same columns were removed from U_0 to produce the matrix U . The reduced data (A of dimension $m \times n$) was constructed with $A = US$.

Multivariate analysis of covariance (ManCova) was used to make inferences about the effects of interest (i.e., to provide P values). In the simplest case of comparing two groups, the ManCova becomes the special case of Hotelling's T^2 test. ManCova does not simply tell one what the difference is. To characterize these differences one usually uses canonical variates analysis (CVA) based upon the parameter estimates from ManCova. CVA is a device that finds the linear combination of the dependent variables (in this case the deformations) that is maximally correlated with the explanatory variables (e.g., male vs. female). In the simple case of one categorical explanatory variable (e.g., sex), this will be the deformation field that best discriminates between males and females. Note that this is not the same as simply subtracting the deformation fields of two groups. This is because 1) the ManCova includes the effects of confounds that are removed, and 2) some aspects of the dimorphic deformations may be less reliable than others (CVA gives deformations that explicitly discount error in relation to predicted differences). The canonical deformations can either be displayed directly as deformation fields, or can be applied to some image to “caricature” the effect detected. In this paper, we combine both in order to illustrate the deformations more clearly.

RESULTS

Tests for significant differences between groups of subjects were performed using a ManCova (see Appendix A) on the deformation parameters. A number of tests were performed, including tests relating to the

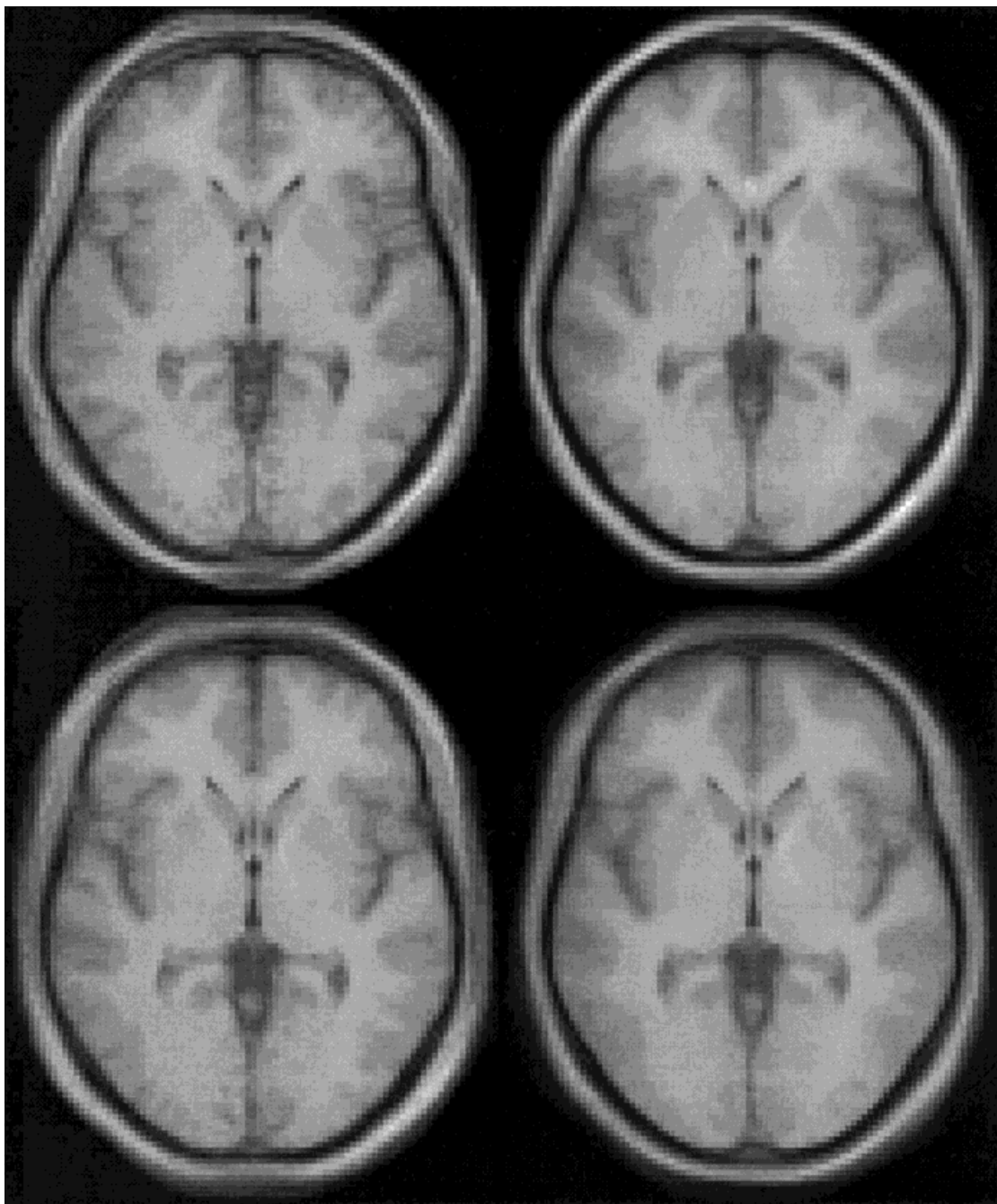


Figure 2.

The mean of the spatially normalized images for each group: left-handed females (**above left**), right-handed females (**above right**), left-handed males (**below left**) and right-handed males (**below right**).

handedness of the subjects, sexual dimorphism, looking at brain asymmetry, and interactions among these factors. A full report of these results will be presented elsewhere. Here we concentrate on a few of the more illuminating analyses.

Handedness, sex, and the interaction between them

A ManCova testing for the effects of both handedness and sex simultaneously suggested extremely sig-

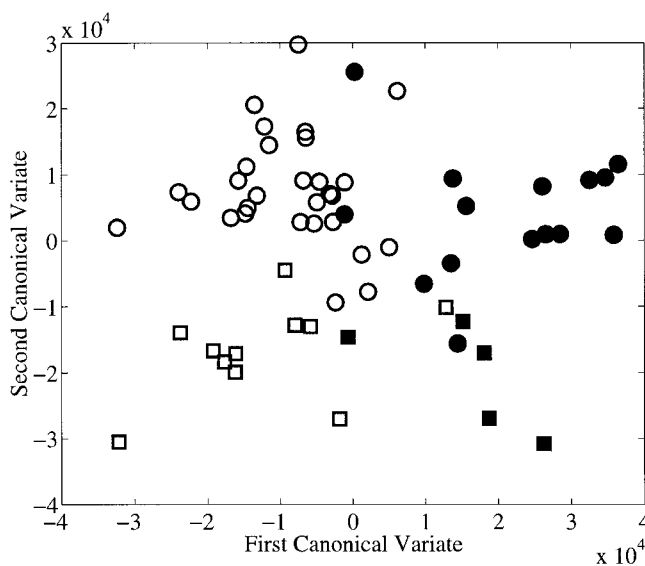


Figure 3.

Separation of subjects using canonical variates analysis. Right-handed females (solid circles), left-handed females (solid squares), right-handed males (open circles), and left-handed males (open squares).

nificant effects ($P = 2.1 \times 10^{-7}$). Because there were two effects of interest, CVA (see Appendix A) could be used to generate a scatter-plot representing the optimum separation of the groups (Fig. 3) in terms of the two corresponding canonical variates. It can be seen that the first canonical variate is mainly sensitive to the differences between men and women, whereas the second discriminates between handedness.

The effects of sex and handedness were then tested individually, both showing significant differences ($P = 0.00014$ and $P = 0.00020$, respectively). The test for sex differences used handedness as a confound, and that for handedness used sex as a confound. A further test failed to show any interaction between handedness and sex ($P = 0.90$). The differences between the groups were characterized using CVA; the results are shown in Figure 4. These can be compared to the difference between brain shapes (after removing confounding effects), as shown in Figure 5. We will comment on the differences between the two sorts of characterization (CVA and those based directly on the parameter estimates) below.

The effect of sex can be most clearly seen in the saggital view, and suggests that men have a more protruding occipital pole, whereas women have more prominent frontal poles. The effect of handedness involves more asymmetric differences affecting predominantly the right frontal lobe (transverse section, Fig. 4, center).

Brain asymmetry

Because the template used by the spatial normalization was symmetrical, it was possible to look at left/right brain asymmetry. The coefficients of the DCT can be divided into those that account for nonlinear deformations that are symmetric, and those that relate to antisymmetric deformations. Very significant brain asymmetries were detected ($P < 0.001$) by testing that the coefficients of the antisymmetric warps differed from zero. Geschwind and Galaburda [1987] discussed many of the asymmetries found by a number of researchers. These include the fact that the left occipital lobe is broader and longer than that on the right, which is confirmed in Figure 5. However, because of the large amount of variability in the occipital lobes, this is not a feature of brain asymmetry that is strongly characterized by CVA (see Fig. 4). Another asymmetry (that was not really confirmed in Geschwind and Galaburda [1987]) is that the right frontal lobe is usually larger than that on the left. However, the results we obtained contradict this finding, in that the left frontal lobe appeared to be the larger of the two. From Figure 5 we see that the magnitude of the difference is relatively small, but it is still a feature that is strongly characterized by CVA. Differences in asymmetry between males and females and between left- and right-handed subjects were both found to be significant ($P = 0.026$ and $P = 0.0076$, respectively), and will be presented elsewhere.

In short, reliable features of asymmetry and dimorphism may not necessarily be the biggest or most obvious. Furthermore, the approach presented here gives estimates of dimorphism that explicitly discount differences due to other factors, in this instance, sex and handedness.

DISCUSSION

In this paper we introduce deformation-based morphometry. This technique allows one to characterize and make inferences about the differences in macroscopic anatomy among structural brain images, and can be seen as the complement to voxel-based morphometry. The latter deals with residual, local differences in tissue compartment composition once the macroscopic differences have been removed. In brief, the parameters describing the mapping of the images to some common template are reduced using singular value decomposition (SVD), and are then subjected to ManCova to provide parameter estimates and statistical inferences. CVA can then be employed to give deformations that best capture the effect one is interested in.

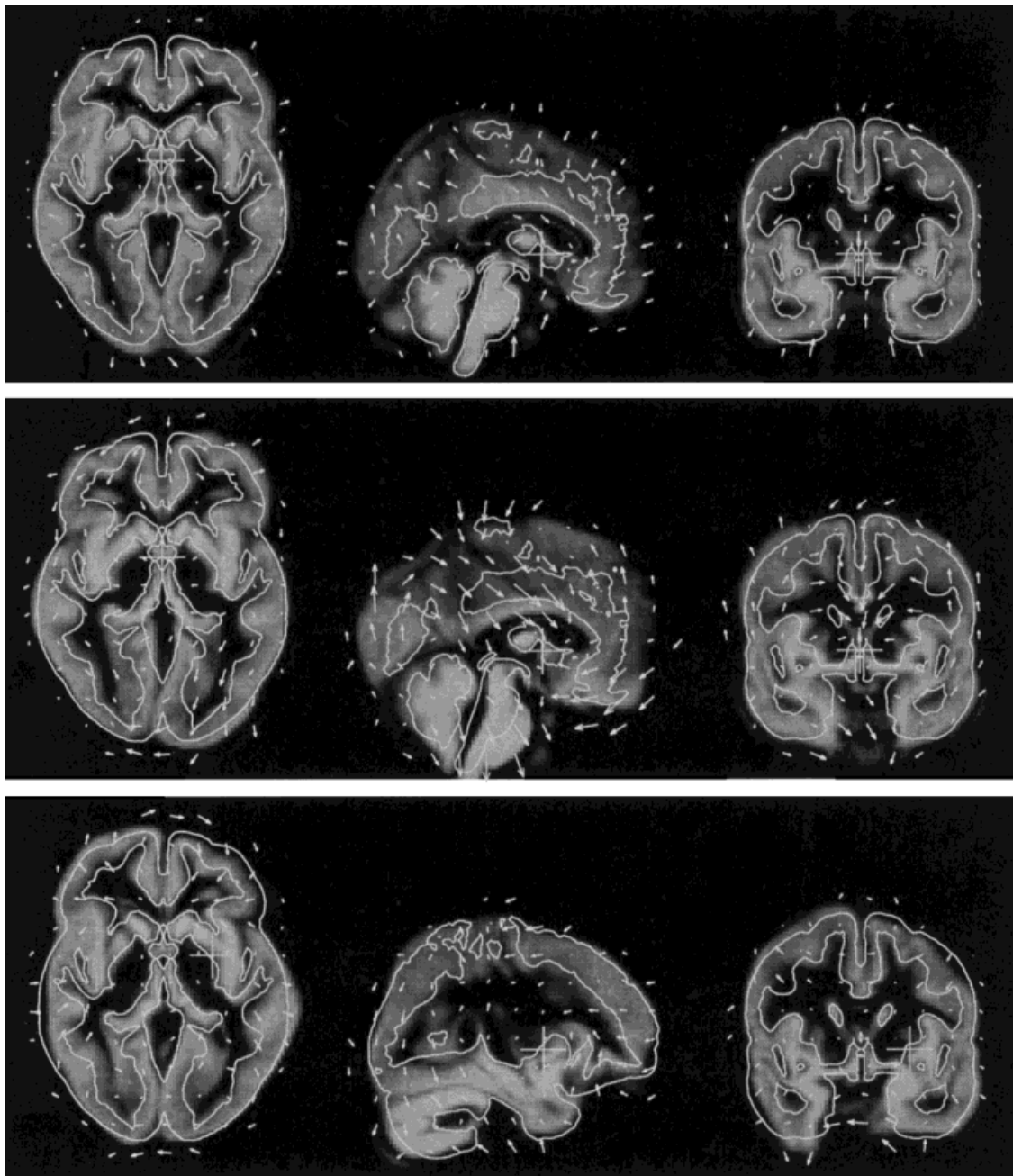


Figure 4.

Nonlinear warps that caricature a male brain (**above**), a right-handed brain (**center**), and natural brain asymmetry (**below**). These have been characterized by canonical variate analysis. The images of grey matter show the caricature of the deformations. Superimposed on this is a contour from the undeformed image. Arrows show the direction of the nonlinear warps characterized by CVA (from undeformed to deformed). Deformations have been arbitrarily scaled for better visualization. These are not the mean differences between brain shapes, but rather the differences that

most clearly distinguish them. In its most general form, CVA produces a set of vectors that best partition the data according to the design matrix. If there are multiple effects of interest, then there is no simple relationship between these effects and the canonical variates, but with only one factor of interest (as in these examples), the canonical variates can be directly related to the factor. In the transverse and coronal sections, the left side of the brain is at left.

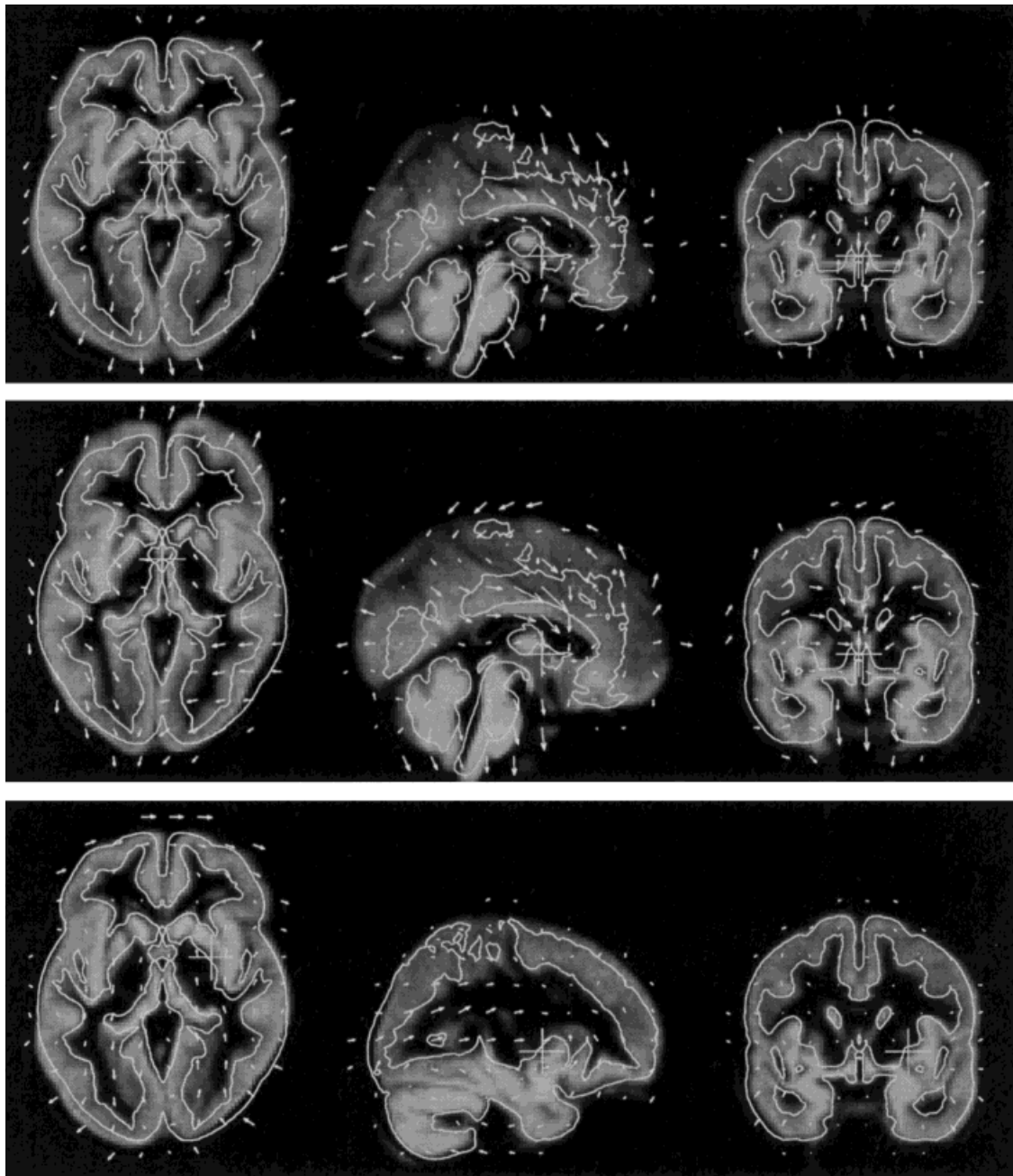


Figure 5.

The deformation required to map from a female to male brain (**above**), left-handed to right-handed brain (**center**), and antisymmetric deformations from a symmetric template to an asymmetric brain (**below**), all multiplied by a factor of 5. The deformations

were computed after first removing the effects of confounds, and are a direct characterization of the parameter estimates without referring to the errors or reliability of the differences (cf. CVA).

We anticipate that the power of this approach will be realized when several explanatory variables are considered together in multifactorial designs. In that case there will be a series of canonical deformations and compounds of explanatory variables that fully charac-

terize the nature of the differences. An intriguing example of this approach would be to examine the effect of being schizophrenic, along with age and the interaction between these factors. This interaction may point to a putative degenerative process in schizophre-

nia that eschews the necessity to acquire longitudinal data (which is very difficult to do). An interaction here would imply that schizophrenic anatomy changes with time at a different rate from that predicted by normal age-related changes.

One important aspect of deformation-based morphometry is that the entire brain is examined in a balanced way. This may be important in the sense that correlated changes in morphology between anatomically connected but distant brain regions will be evident in a way that would be missed by just looking at one easily identified structure. In terms of characterizing the effects, we have used CVA and the parameter estimates directly (i.e., differences having adjusted for confounds). The latter approach is a special case, due to having just one effect of interest, i.e., of using the eigenvectors of the fitted effects. This is an alternative to CVA which uses the generalized eigenvectors of the fitted effects and error. Both are useful characterizations and can be used to complement each other: the simple eigenvectors show which warps are the biggest, whereas the canonical vectors give effects that are more reliable.

The current study has some features in common with that of Bookstein [1997]. Both used multivariate statistics to differentiate between the brain shapes of different populations. The measure of shape used by the two studies was also similar. However, the methods differ principally in that the current approach utilizes the more general statistical method of Man-Cova, rather than the special case of Hotelling's T^2 test. In addition, the estimates of shape were based upon the whole brain, rather than on a two-dimensional section through the corpus callosum, and were identified automatically rather than by reliance upon manual landmark identification.

There are many features of deformation fields that could be used to characterize differences in brain shape, and so could be included in such tests. In principle, the Jacobians of the transformations (a matrix field relating to the spatial derivatives of the transformation) should be more reliable indicators of brain shape than absolute deformations (since absolute deformations need to be quantified relative to some arbitrary reference position). One simple feature of a Jacobian that could be considered is the determinant, which directly encodes the relative volume of a brain region. With more sophisticated Bayesian image registration methods, more control is exerted over the nature of the distributions from which the parameters are drawn. The parameter estimates may no longer be normally distributed, so simple tests based upon assumptions of normality would not be appropriate. It

is envisaged that future work on morphometry should develop in concurrence with the methods used for estimating the deformations. The parameter distributions imposed upon the deformations by the registration method could be used in morphometry studies. Similarly, knowledge of the variability of brain shapes obtained from morphometry could be used as a priori information for Bayesian image registration methods. Both fields would clearly benefit by having a compact and concise representation of the anatomical variability of brains.

Cao and Worsley [1997] and Cao et al. [1997] also described a multivariate approach to morphometry. This approach belongs to the voxel-based morphometry class, in that the multivariate inferences are about regionally specific differences (therein producing statistical parametric map (SPM)) and address things like displacement of the cortical surface from some normal position. In this instance, the multivariate nature of the analyses pertains to the vectorial displacements at each voxel, and not to the vector-fields that subsume all voxels. Approaches such as this and the one described in our study speak to an exciting and progressive refinement of computational neuroanatomy in imaging neuroscience.

ACKNOWLEDGMENTS

The authors thank all the fellows at the Wellcome Department of Cognitive Neurology who (knowingly or otherwise) provided data for this project.

REFERENCES

- Altshuler LL, Casanova MF, Goldberg TE, Kleinman JE (1990): The hippocampus and parahippocampus in schizophrenia, suicide, and control brains. *Arch Gen Psychiatry* 47:1029–1034.
- Ashburner J, Friston KJ (1998): Nonlinear spatial normalization using basis functions. *Hum Brain Mapp*
- Ashburner J, Neelin P, Collins DL, Evans AC, Friston KJ (1997): Incorporating prior knowledge into image registration. *Neuroimage* 6:344–352.
- Bartzokis G, Nuechterlein KH, Marder SR, Mintz J, Dery K, Laack K (1996): Age at illness onset and left temporal lobe length in males with schizophrenia. *Psychiatry Res* 67:189–201.
- Blackwood DH, Young AH, McQueen JK, Martin MJ, Roxborough HM, Muir WJ, St. Clair DM, Kean DM (1991): Magnetic resonance imaging in schizophrenia: Altered brain morphology associated with P300 abnormalities and eye tracking dysfunction. *Biol Psychiatry* 30:753–769.
- Bookstein FL (1997): Landmark methods for forms without landmarks: Morphometrics of group differences in outline shape. *Med Image Analysis* 1:225–243.
- Cao J, Worsley KJ (1997): The geometry of the Hotelling's T^2 random field with applications to the detection of shape changes. *Ann Stat*.

- Cao J, Worsley KJ, Liu C, Collins L, Evans AC (1997): New statistical results for the detection of brain structural and functional change using random field theory. *Neuroimage* 5:512.
- Ciesielski KT, Knight JE (1994): Cerebellar abnormality in autism: A nonspecific effect of early brain damage? *Acta Neurobiol Exp (Warsz)* 54:151–154.
- Crow TJ (1990): Temporal lobe asymmetries as the key to the etiology of schizophrenia. *Schizophr Bull* 16:433–443.
- Frazier JA, Giedd JN, Kayser D, Albus K, Hamburger S, Alaghband-Rad J, Alaghband-Rad JL, Lenane MC, McKenna K, Breier A, Rapoport (1996): Childhood-onset schizophrenia: Brain MRI rescan after 2 years of clozapine maintenance treatment. *Am J Psychiatry* 153:564–566.
- Friston KJ, Frith CD, Frackowiak RSJ, Turner R (1995a): Characterizing dynamic brain responses with fMRI: A multivariate approach. *Neuroimage* 2:166–172.
- Friston KJ, Ashburner J, Frith CD, Poline JB, Heather JD, Frackowiak RSJ (1995b): Spatial registration and normalization of images. *Hum Brain Mapp* 2:165–189.
- Gaffney GR, Kuperman S, Tsai LY, Minchin S (1989): Forebrain structure in infantile autism. *J Am Acad Child Adolesc Psychiatry* 28:534–537.
- Geschwind N, Galaburda AM (1987): Cerebral Lateralization, Biological Mechanisms, Associations and Pathology, Cambridge, MA: MIT Press, pp 21–34.
- Jacobsen LK, Giedd JN, Vaituzis AC, Hamburger SD, Rajapakse JC, Frazier JA, Kayser D, Lenane MC, McKenna K, Gordon CT, Rapoport JL (1996): Temporal lobe morphology in childhood-onset schizophrenia. *Am J Psychiatry* 153:355–361.
- Krzanowski WJ (1988): Principles of Multivariate Analysis—A Users Perspective. Oxford University Press, New York.
- Lieberman J, Bogerts B, Degreef G, Ashtari M, Lantos G, Alvir J (1992): Qualitative assessment of brain morphology in acute and chronic schizophrenia. *Am J Psychiatry* 149:784–794.
- Murphy DG, DeCarli C, Daly E, Haxby JV, Allen G, White BJ, McIntosh AR, Powell CM, Horwitz B, Rapoport SI (1993): X-chromosome effects on female brain: A magnetic resonance imaging study of Turner's syndrome. *Lancet* 342:1197–1200.
- Nasrallah HA, Schwarzkopf SB, Olson SC, Coffman JA (1990): Gender differences in schizophrenia on MRI brain scans. *Schizophr Bull* 16:205–210.
- Noga JT, Aylward E, Barta PE, Pearlson GD (1995): Cingulate gyrus in schizophrenic patients and normal volunteers. *Psychiatry Res* 61:201–208.
- Nopoulos P, Torres I, Flaum M, Andreasen NC, Ehrhardt JC (1995): Brain morphology in first-episode schizophrenia. *Am J Psychiatry* 152:1721–1723.
- Reiss AL, Mazzocco MM, Greenlaw R, Freund LS, Ross JL (1995): Neurodevelopmental effects of X monosity: A volumetric imaging study. *Ann Neurol* 38:731–738.
- Suddath RL, Christison GW, Torrey EF, Casanova MF, Weinberger DR (1990): Anatomical abnormalities in the brains of monozygotic twins discordant for schizophrenia. *N Engl J Med* 322:789–794.
- Tsai LY, Jacoby CG, Stewart MA (1983): Morphological cerebral asymmetries in autistic children. *Biol Psychiatry* 18:317–327.
- Wright IC, McGuire PK, Poline JB, Travers J, Murray RM, Frith CD, Frackowiak RSJ, Friston KJ (1995): A voxel-based method for the statistical analysis of gray and white matter density applied to schizophrenia. *Neuroimage* 2:244–252.

APPENDIX A

Multivariate analysis of covariance and canonical variates analysis

The analysis may be confounded by a number of possible effects. For the analysis described here, the confounds are modeled by an $m \times g$ design matrix G . Each column of G can be a vector of covariates, or alternatively can be arranged in blocks for group-specific estimation. The mean is removed from the data by including a constant column in G . Any variance in the data ($m \times n$ matrix A) that could be attributed to the confounds is removed by:

$$A_a = A - G(G^T G)^{-1} G^T A.$$

Similarly, the effects of interest are modeled by an $m \times c$ design matrix C . The columns in this design matrix are orthogonalized with respect to matrix G :

$$C_a = C - G(G^T G)^{-1} G^T C.$$

The ManCova involves assessing how the predictability of the observed deformation parameters change when the effects of interest are discounted. This involves the distributions of the residuals that are assumed to be multinormal. The statistic is related to the determinants of the covariance matrices describing these distributions. In practice, the residual sum of squares and products (SSP) matrix, (W_0), is compared to the SSP matrix of the fitted effects (B_0). These matrixes are obtained by:

$$T = C_a ((C_a^T C_a)^{-1} C_a^T A_a)$$

$$B_0 = T^T T$$

$$W_0 = (A_a - T)^T (A_a - T).$$

The statistic is called Wilk's lambda (Λ), and is based upon the ratios of the determinants (see Krzanowski [1988] for a more detailed explanation):

$$\Lambda = \frac{|W_0|}{|B_0 + W_0|}.$$

This statistic is transformed to a χ^2 statistic (with nc degrees of freedom under the null hypothesis) using the approximation of Bartlett:

$$\chi^2 \approx ((n - c + 1)/2 - (m - c - g)) \log_e(\Lambda).$$

Finally, the cumulative χ^2 distribution function is used to make inferences about whether the null hypothesis

(that there is no difference between the distributions) can be rejected.

Canonical variates analysis (CVA) can be used to characterize any effects of interest. The vectors that best discriminate between the groups are obtained from the c eigenvectors of B_0 (e.g., differences in Fig. 5) or $W_0^{-1}B_0$ (i.e., the canonical vectors ϵ in Fig. 4) that have nonzero eigenvalues. The corresponding canonical variates are given by $A_a\epsilon$.

APPENDIX B

Partitioning the deformation fields into positional size, and shape components

The deformation fields are defined by both nonlinear and affine components. In order to proceed, it is necessary to decompose the transformation into components relating to position and size (uninteresting components), and shape (the components that we are interested in). In order to effect this decomposition, each deformation field was reconstructed from its parameters. Each field provides a mapping from points in the template to points in the image, allowing standard landmark-based registration methods to be used to extract size and positional information. Rather than basing the registration on a few landmarks, all the elements of the deformation field corresponding to voxels within the brain were considered (by weighting with the image shown in Fig. 1). This involved first determining the translations by computing centers of mass:

$$\bar{x} = \frac{\sum_{i=1}^I x_i w_i}{\sum_{i=1}^I w_i}$$

$$\bar{y} = \frac{\sum_{i=1}^I y_i w_i}{\sum_{i=1}^I w_i}$$

where x_i is the coordinate of the i th voxel of the template, y_i is the location that it maps to, and w_i is the weighting for that element. The rotations were computed from the cross-covariance matrix (C) between the elements and deformed elements (after removing the effects of position):

$$c_{j,k} \propto \sum_{i=1}^I w_i (x_{i,j} - \bar{x}_j)(y_{i,k} - \bar{y}_k).$$

The 3×3 matrix C was decomposed using singular value decomposition to give three matrixes, U , S , and V (such that $C = USV^T$, where U and V are unitary, and S is a diagonal matrix). The rotation matrix (R) could then be reconstituted from these matrixes by $R = UV^T$. Finally, moments around the centers were used to correct for relative size differences (z):

$$z = \sqrt{\frac{\sum_{j=1}^3 \sum_{i=1}^I (x_{i,j} - \bar{x}_j)^2 w_i}{\sum_{j=1}^3 \sum_{i=1}^I (y_{i,j} - \bar{y}_j)^2 w_i}}.$$

After removing the effects of translation, rotation, and scaling from the deformation fields, they were then reparameterized by the lowest frequency coefficients of their three-dimensional DCTs.